Three-Dimensional Turing Structures and Spatial Solitons in Optical Parametric Oscillators

K. Staliunas

Physikalisch Technische Bundesanstalt, 38116 Braunschweig, Germany

(Received 1 December 1997)

An order parameter equation is derived for degenerate optical parametric oscillators in the form of a three-dimensional Swift-Hohenberg equation. Three-dimensional Turing structures (lamellae and tetrahedral patterns) and three-dimensional spatial solitons (dark spherical bubbles) are predicted as stable structures. [S0031-9007(98)06416-3]

PACS numbers: 42.65.Sf, 42.60.Mi, 42.65.Tg, 47.54.+r

Substantial progress has been achieved in the last decade in understanding transverse pattern formation in lasers and other nonlinear optical systems. Order parameter equations have been derived for lasers [1,2], externally driven nonlinear resonators [3], optical parametric oscillators (OPOs) [4,5], and photorefractive oscillators [6], joining nonlinear optical systems to general macroscopic pattern formation physics. Turing patterns [7] (tilted waves [8], stripe patterns, hexagons [3], and cross roll structures [9]) have been predicted, some of them already experimentally observed [10]. Besides spatially extended Turing patterns, spatially confined Ising structures (in nonlinear optics usually called "spatial localized structures") exist in nonlinear optical systems. These are optical vortices (dark topological solitons) [11] and spatial bright solitons [12].

These structures were found and investigated predominantly in two-dimensional (2D) systems, where the fields depend on two transverse spatial coordinates and evolve slowly in time. A single longitudinal mode family is considered in the theoretical models, where the fields are assumed to change negligibly along the resonators. Little is known about three-dimensional spatial light structures—fields associated with the simultaneous emission of large numbers of longitudinal and transverse modes. Some analysis of 3D Turing structures has been given in [13] for nonoptical systems, and in [14] for lasers.

Multilongitudinal mode emission can occur in lasers and other nonlinear optical systems when the gain line is broader than the free spectral range of the resonator. The gain line for OPOs (the line of phase synchronism) is usually very broad, therefore this system is suited for generating 3D structures. In particular, we analyze here concretely degenerate OPOs (DOPOs), restricting other nonlinear optical systems to a short discussion in the conclusions.

For simplicity, we discuss a synchronously pumped DOPO as sketched in Fig. 1. The 3D subharmonic pulses travel around the resonator filled with a medium with second order nonlinearity, feeding from the energy of a sequence of pump pulses. The pump pulses are not resonant. The 3D structures are expected to reside within the propagating subharmonic pulses. We show in this Letter that the spatiotemporal dynamics of the field within the resonating pulses is described by a 3D Swift-Hohenberg equation (SHE). We analyze 3D Turing and Ising structures which are solutions of the derived order parameter equation.

The model of a synchronously pumped DOPO is used for simplicity only. It includes pump pulses of infinitely long duration, which corresponds to continuous pumping. The analysis applies for both synchronously and continuously pumped DOPOs.

Interaction of the three-dimensional slowly varying envelopes of the 3D subharmonic and pump pulses, $A_1(\vec{r}_\perp, \tau, z)$ and $A_0(\vec{r}_\perp, \tau, z)$, respectively, is described by the following equations:

$$\frac{\partial A_1}{\partial z} = (\nu_1 - \nu_0)\frac{\partial A_1}{\partial \tau} + id_{\mathrm{II},1}\frac{\partial^2 A_1}{\partial \tau^2} + id_{\perp,1}\nabla_\perp^2 A_1 + \chi A_0 A_1^*, \tag{1a}$$

$$\frac{\partial A_0}{\partial z} = id_{\mathrm{II},0}\frac{\partial^2 A_0}{\partial \tau^2} + id_{\perp,0}\nabla_\perp^2 A_0 - \chi A_1^2. \tag{1b}$$

Here, $\nu_j = \partial k_j/\partial\omega_j$ are the group velocities for the pump ($j = 0$) and subharmonic ($j = 1$) waves, $d_{\mathrm{II},j} = \partial^2 k_j/\partial\omega_j^2$ are longitudinal dispersion coefficients, $d_{\perp,j} = 1/2k_j$ are transverse diffraction coefficients, and χ is the nonlinear coupling coefficient. Evolution occurs along the longitudinal coordinate z. Fields are defined in the transverse 2D space $\vec{r}_\perp = (x, y)$, ($\nabla_\perp^2 = \partial^2/\partial x^2 + \partial^2/\partial y^2$),

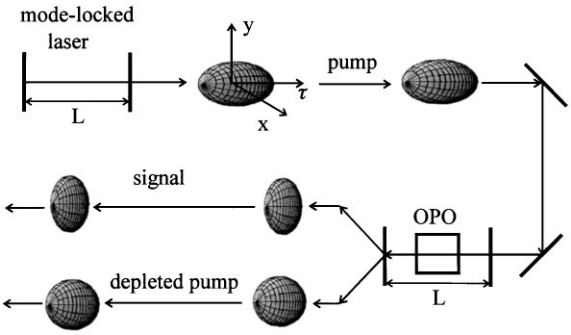

FIG. 1. Scheme of synchronously pumped degenerate optical parametric oscillator.

and in the longitudinal space τ (τ is a retarded time in a frame propagating with the group velocity of the pump pulses).

The changes of the fields during one resonator round-trip are assumed to be small. This allows one, first, to obtain a mapping describing the discrete changes of the subharmonics pulse in successive resonator round-trips. Second, it allows one to replace the discrete mapping by a continuous evolution, thus to obtain the order parameter equation in the form of a partial differential equation.

Diffractive and dispersive changes on the pump are neglected for the propagation over the crystal length Δl, which is assumed small compared to the total length of the resonator L. Assuming that the subharmonic changes negligibly along the crystal $A_1(\vec{r}_\perp, \tau, z) \approx A_1(\vec{r}_\perp, \tau)$, Eq. (1b) can be integrated: $A_0(\vec{r}_\perp, \tau, z) = A_0(\vec{r}_\perp, \tau, 0) - \chi A_1^2(\vec{r}_\perp, \tau) z$. The mean value of the pump envelope is

$$A_0(r_\perp, \tau, z) = A_0(\vec{r}_\perp, \tau, 0) - \chi A_1^2(\vec{r}_\perp, \tau)\Delta l/2 . \quad (2)$$

.

This approximation of mean pump value (2) allows one to obtain a mapping of the subharmonic pulse in successive resonator round-trips. Taking into account the nonlinear interaction in the crystal (1a), diffractive propagation in a resonator, losses on the mirrors $-\alpha_1$, and the phase shift $\Delta\varphi$ due to resonator length detuning, the following mapping results:

$$A_{1,(n+1)} = A_{1,(n)} + (\nu_1 - \nu_0)\Delta l \frac{\partial A_1}{\partial \tau} + i\Delta\varphi A_{1,(n)} - \alpha_1 A_{1,(n)} + i d_{\mathrm{II},1}\Delta l \frac{\partial^2 A_1}{\partial \tau^2} + i d_{\perp,1} L \nabla_\perp^2 A_1 + \chi \Delta l [A_0 - \chi(\Delta l/2) A_1^2] \cdot A_1^* . \quad (3)$$

Dispersion is assumed to occur in the nonlinear crystal only. Diffraction is assumed to occur throughout the propagation over the whole resonator length L.

Transforming the mapping (3) into a continuous evolution in time t ($t = nL\alpha_1/c$ is normalized to the photon lifetime in the resonator), and, renormalizing the fields, one obtains

$$\frac{\partial A}{\partial t} = P \cdot A^* - A + i(\nabla^2 + \Delta)A - |A|^2 A , \quad (4)$$

which is a parametrically driven Ginzburg-Landau equation similar to that obtained for the corresponding problem in 2D [4,5]. Here, the following variable transformations were used: $P(\vec{r}_\perp, \eta) = A_0(\vec{r}_\perp, \eta, 0)\chi\Delta l/\alpha_1$, $A(\vec{r}_\perp, \tau, \eta) = A_1(\vec{r}_\perp, \eta, t) \cdot \chi \cdot \Delta l/\sqrt{2}$, $X, Y = x, y\sqrt{\alpha_1/(d_\perp L)}$, $\eta = \tau\sqrt{(\alpha_1/(d_{\mathrm{II}}\Delta l)}$, $\Delta = \Delta\varphi/\alpha_1$. The 3D Laplace operator $\nabla^2 = \partial^2/\partial X^2 + \partial^2/\partial Y^2 + \partial^2/\partial\eta^2$ is calculated in a coordinate frame propagating with the subharmonic pulse: $\vec{r} = (X, Y, \eta)$.

A further simplification of (4) is possible for a pump value close to generation threshold ($|P - 1| \ll 1$). This can be done by adiabatically eliminating the small imaginary part of the field, such as, e.g., in [4]. Applying directly the derivation procedure of the 2D case from [4] to the 3D parametrically driven Ginzburg-Landau equation, one obtains

$$\frac{\partial A}{\partial t} = (P - 1)A - \frac{1}{2}(\nabla^2 + \Delta)^2 A - A^3, \quad (5)$$

which is a real SHE in 3D.

The spatiotemporal structure of the pump pulses are incorporated in $P(\vec{r})$; therefore Eq. (5) is valid both for synchronously or continuously pumped OPOs. For the lateral coordinates, the boundary conditions have to correspond to experiments: For example, the aperture in a resonator implies zero boundaries; infinitely broad aperture (and pump profile) systems require no lateral boundaries at all. In the longitudinal direction, periodic boundaries are to be used, corresponding to periodic repetition of pattern.

Further, in the analytical treatment of patterns, a homogeneous pump in 3D is assumed. This assumption is legitimate when the typical size of spatial structures is much smaller than the spatial size of pump pulses. This occurs for sufficiently broad pump beams ($|\partial P/\partial X|, |\partial P/\partial Y| \ll |P|$), and also for sufficiently long pump pulses ($|\partial P/\partial\eta| \ll |P|$). Under this condition, one can scale out the pump parameter, and write (5) in the form

$$\frac{\partial A}{\partial t} = A - (\nabla^2 + \Delta)^2 A - A^3, \quad (6)$$

having only one free parameter—the detuning Δ.

The correctness of the linear part of (5) can be tested by comparison of the Liapunov growth exponent spectra calculated for (5), with the round-trip increments of the fields calculated for (1) and (2). It follows from this comparison that (5) describes the linear pattern forming properties (transverse wave number selection) of the DOPO well not only near the threshold: $(P - 1) \ll 1$, where (5) is strictly mathematically valid, but also moderately above the threshold $(P - 1) \approx 1$.

In the limit of small detuning, a stable solution of the 3D SHE (6) is a homogeneous distribution with amplitude $|A| = \pm\sqrt{1 - \Delta^2}$, and one of the two phase values: $\varphi = 0, \pi$. However, in a transient stage of evolution, when starting from random field distributions, the subharmonic field can consist of separated domains, with one of two phase values. The phase domains in 2D patterns are separated by domain boundaries—dark switching waves,

as analyzed in [15]. Analogously, similar 3D domains should exist, separated by 2D domain walls.

A numerical integration of SHE (6) was performed to test the idea of domains in 3D. (A split-step technique was used on a spatial grid of $32 \times 32 \times 32$.) The result is given in Fig. 2 for a particular time in the transient evolution. Two domains of uniform phase embedded in the background of the opposite uniform phase are apparent.

The dynamics of the 3D domains depends on the detuning parameter in a similar way to that of 2D domains [15]. Negative, or small positive, detuning leads to contraction and eventual disappearance of domains. Large positive detuning leads to the growth of domains and formation of a "labyrinth" structure, as discussed below. However, in a particular detuning range, the contracting domains can stabilize to a particular size. One obtains then spherically symmetric stable "bubbles," which are the localized structures (spatial solitons) of the 3D SHE. Such an ensemble of stable bubbles is shown in Fig. 3, as obtained numerically.

The stability limits of the spatial localized structures was analyzed by solving the 3D SHE (6) numerically. The 3D solitons are stable in the interval $0.430 \pm 0.001 < \Delta < 0.460 \pm 0.001$. This stability range is narrower than that of the corresponding dark rings in 2D, which is $0.287 \pm 0.001 < \Delta < 0.460 \pm 0.001$ [15].

Large detuning values lead to Turing structures—structures with a dominating nonzero spatial wave number $|\vec{k}| = \sqrt{\Delta}$. In 2D, a parallel stripe pattern is such a Turing pattern: $A(\vec{r}) \approx \sqrt{4/3}\cos(\vec{k}\vec{r})$. A direct continuation to the 3D case gives the analog of stripe patterns—a standing wave pattern (also called "lamellae"). However, besides lamellae another stable Turing structure is possible in 3D [a structure made up of four resonant standing waves, directed as illustrated in Fig. 4(a)]; $A(\vec{r}) \approx \sum_{j=1,4}(A_j e^{i\vec{k}_j\vec{r}} + \text{c.c.})$. The four $\vec{k}$-resonant standing waves $|\vec{k}_j| = \sqrt{\Delta}$ do not lie in the same plane; thus such a tetragonal structure can exist only in 3D space. The phases of the four nonplanar standing waves with complex amplitudes $A_j = |A_j|e^{\varphi_j}$ obey $\sum_{j=1,4}\varphi_j = \pi$.

Stability analysis shows that both the lamellae and the tetragonal structures are stable. For stability analysis a variational potential for (6) was calculated: $F = \int(-A^2/2 + A^4/4)\cdot d\vec{r}$. (Laplace operators do not appear in the potential, if we deal with the $\vec{k}$-resonant structures.) Calculation of the variational potential yields the potential minima associated with these structures in the parameter space of A_j. The minimum values of potential are $F_l = -\frac{1}{16} = -0.1666\ldots$ for lamellae, and $F_4 = -\frac{2}{15} = -0.1333\ldots$ for the tetragonal structure. Lamellae are thus more stable than the tetragonal structure. For comparison, the 3D continuation of the resonant square and of the hexagonal patterns have potentials $F_2 = -\frac{1}{10} = -0.1$, and $F_3 = -\frac{1}{9} = -0.111\ldots$, respectively; however, these unstable patterns correspond not to local potential minima in the parameter space of A_j but to saddle points.

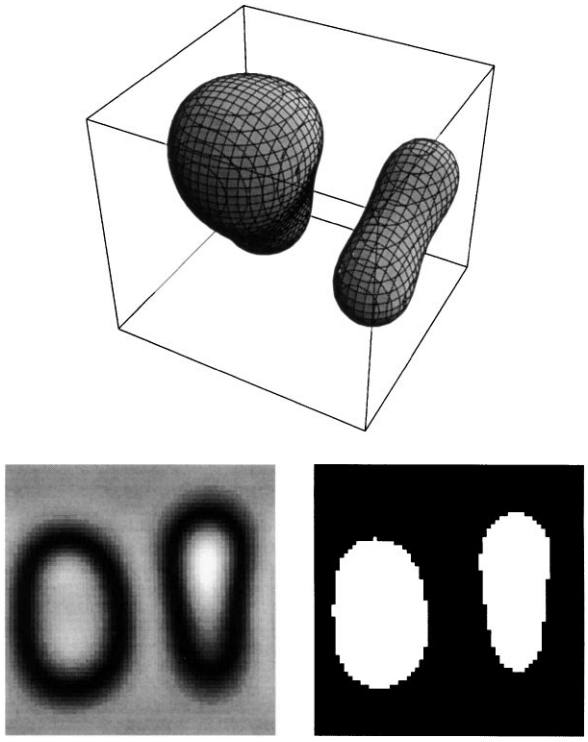

FIG. 2. Phase domains as obtained by numerical integration of the 3D SHE (6) depicted by surfaces of zero field. Below, a 2D cut is given showing the field intensity (left) and the field phase (right). Detuning $\Delta = 0.4$. Periodic boundaries are used on the box with a size of $\Delta x = \Delta y = \Delta\eta = 20$.

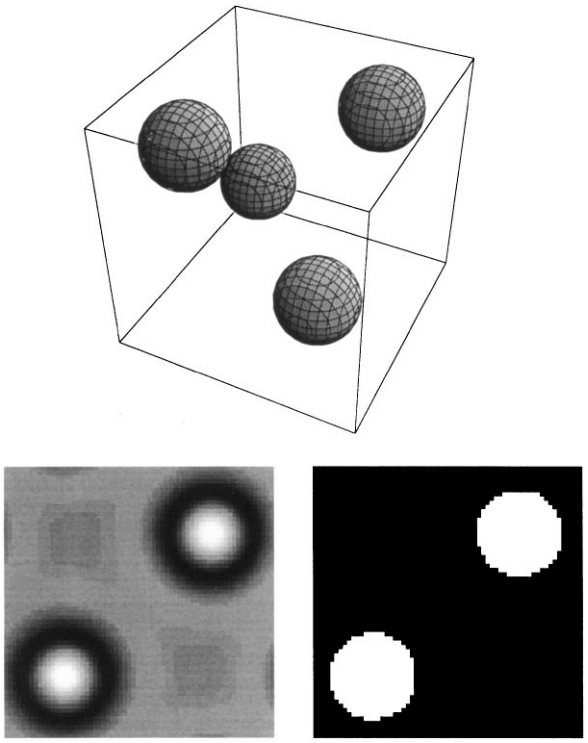

FIG. 3. Localized structures (stable bubbles). Conditions as in Fig. 2, except detuning $\Delta = 0.45$.

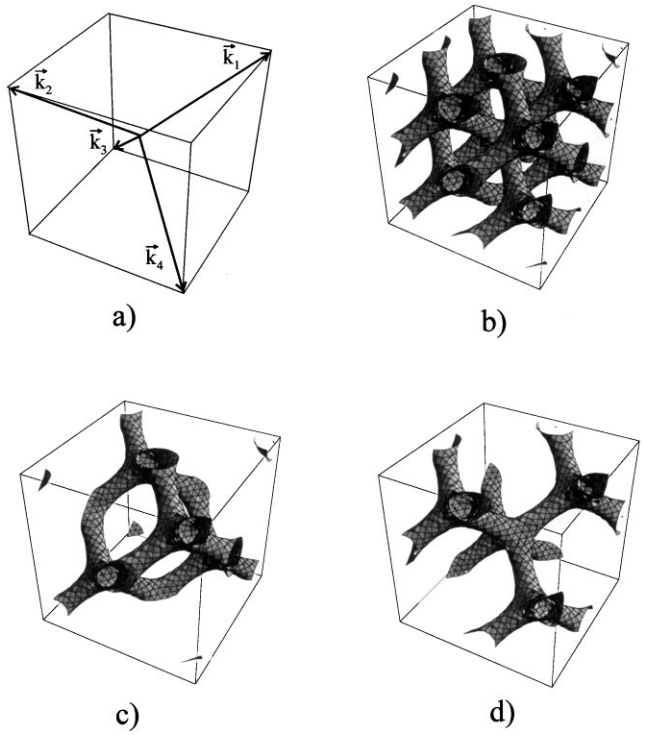

FIG. 4. $\vec{k}$-resonant wave vectors forming the tetragonal structure (a). The isolines at 85% of maximum field intensity (b), at 93% (c), and at -93% (d) of maximum amplitudes as obtained by numerical integration of 3D SHE (6) for $\Delta = 1.2$, and for the box size $\Delta x = \Delta y = \Delta\eta = 10$.

Numerical integration of SHE (6) confirms the stability of the tetragons. The numerical results are given in Fig. 4(b), by the isolines at 85% of the maximum field intensity. This intensity structure consists actually of two nested structures given in Figs. 4(c) and 4(d), where the isosurfaces at $+93\%$ and -93% of the amplitudes are plotted.

In conclusion, we summarize as follows.

(1) Tunability of a broad gain band system.—A DOPO has a broad gain line width (the line of phase synchronism), typically by many orders of magnitude larger than the free spectral range of the resonator. Nevertheless, the variation of the resonator length (on a scale of the optical wavelength) allows the changing of the detuning parameter in (5), thus allowing the manipulation of the 3D structures.

This seeming paradox can be understood in the following way. The maximum gain for a plane wave of subharmonics occurs when its phase has a particular value $\varphi = 0, \pi$ with respect to the pump phase at the entrance of the nonlinear crystal. Tuning of the resonator length breaks the optimum phase relation for the plane wave. Therefore a modulation in the subharmonic field should appear, causing a Guoy phase shift, which brings the phase to its optimum value. (The Guoy phase shift is proportional to the spatial wave number of the appearing modulation). This modulation can appear in the transverse, in the longitudinal, or in both directions simultaneously, resulting in oblique lamellae or tetragonal structures.

(2) *Analogy between 2D and 3D cases.*—The order parameter equation derived here for a 3D DOPO is analogous to that derived for DOPOs in the 2D case [4]. This suggests that this analogy between 2D and 3D systems is valid not only for DOPOs, but also for other nonlinear optical systems. A requirement is that nonlinear processes should be fast, compared with the time of light propagation over typical length scales of longitudinal modulation. Then the order parameter equations derived for other nonlinear optical systems in 2D (e.g., externally driven nonlinear resonators containing focusing-defocusing media, or saturable absorbers [3]), can be straightforwardly extended to the 3D case. Instead of Turing or Ising structures in 2D, one should obtain then the corresponding 3D structures cyclically propagating in the resonator.

The 3D extension of equations results in corresponding 3D extension of the structures. The 3D structures having direct counterparts in 2D are as follows: phase domains, localized structures in the form of "bubbles," and lamella structures. However, the family of 3D structures is richer than that of 2D. An example of such a specific 3D structure not having a counterpart in 2D is the resonant tetragonal pattern, which is supported by a cubic nonlinearity.

Discussions with C. O. Weiss, G. Slekys, V. Sirutkaitis, R. Grigonis, and R. McDuff are acknowledged. This work has been supported by Deutsche Forschungsgemeinschaft, and NATO Grant No. HTECH.LG 970522.

[1] K. Staliunas, Phys. Rev. A **48**, 4847 (1993).
[2] J. Lega, J. V. Moloney, and A. C. Newell, Phys. Rev. Lett. **73**, 2978 (1994).
[3] P. Mandel, M. Georgiou, and T. Erneux, Phys. Rev. A **47**, 4277 (1993).
[4] K. Staliunas, J. Mod. Opt. **42**, 1261 (1995).
[5] S. Longhi and A. Geraci, Phys. Rev. A **54**, 4581 (1996).
[6] K. Staliunas, M. F. H. Tarroja, G. Slekys, C. O. Weiss, and L. Dambly, Phys. Rev. A **51**, 4140 (1995).
[7] A. Turing, Philos. Trans. R. Soc. London B **237**, 37 (1952).
[8] P. K. Jakobsen, J. V. Moloney, A. C. Newell, and R. Indik, Phys. Rev. A **45**, 8129 (1992).
[9] K. Staliunas and C. O. Weiss, Physica (Amsterdam) **81D**, 79 (1985).
[10] K. Staliunas, G. Slekys, and C. O. Weiss, Phys. Rev. Lett. **79**, 2658 (1997).
[11] P. Coullet, L. Gil, and F. Rocca, Opt. Commun. **73**, 403 (1989); C. Tamm and C. O. Weiss, Opt. Commun. **78**, 253 (1990).
[12] P. Coullet and K. Emilson, Physica (Amsterdam) **188A**, 190 (1992); S. Fauve and O. Thual, Phys. Rev. Lett. **64**, 282 (1990).
[13] A. De Wit, G. Dewel, P. Borcmans, and D. Walgraef, Physica (Amsterdam) **61D**, 289 (1992).
[14] N. L. Komarova, B. A. Malomed, J. V. Moloney, and A. C. Newell, Phys. Rev. A **56**, 803 (1997).
[15] K. Staliunas and V. J. Sanchez-Morcillo, Phys. Rev. A **57**, 1454 (1998); Phys. Lett. A **241**, 28 (1998).